Thermal properties of colloidal Ag nanoparticles prepared by UV irradiation method

E. SHAHRIARI[a,b,*], G. SHAMS[c]
[a]*Shahid Mohajer, Faculty of Isfahan, Technical and vocational university, Isfahan, Iran*
[b]*Department of Physics, Faculty of Science, Shahrekord University, Shahrekord, Iran*
[c]*Department of Engineering, Shahrekord Universiti, Shahrekord, Iran*

In this article, thermal diffusivity of Ag nanoparticles prepared by UV-irradiation technique was measured. It was found that by increasing UV irradiation time the size of particles decreased. The X-ray diffraction pattern indicates the presence of crystalline Ag and the average grains size were obtained in the range of 5 to18 nm. The thermal diffusivity of the prepared samples was measured by standard dual beam mode mismatched thermal lens technique. The results showed that the value of thermal diffusivity increases with increasing the particles size. We have explained our finding by phonon scattering at interface of particles and surrounded liquid.

(Received November 16, 2017; accepted February 12, 2019)

Keywords: Thermal Lens, Nanoparticles, Thermal diffusivity, UV irradiation

1. Introduction

Metal nanoparticles because of their unique properties find many applications in optical components, electronics, medical therapies and heat transfer fluids in automotive electronic cooling [1-7]. The laser excitation of fluids containing metal nanoparticles, generates hot electrons on the surface of particles, which could increase the thermal diffusivity of fluid through electron phonon scattering. Ag nanoparticles can be prepared by many physical and chemical methods [8-10]. On the other hand, and among the physical methods the UV irradiation, it can be found one of the most successful ones to synthesize Ag nanoparticles [11]. One of the advantages of this method is controlling the size of particles by UV irradiation time.

There are many photothermal techniques for measuring thermal diffusivity of a nanofluid, but thermal lens (TL) technique is the most sensitive and reliable one, which is based on temperature gradient due to absorption of optical radiation and subsequent nonradiative relaxation of the excited molecules [12-16]. Thermal conductivity, and hence, the thermal diffusivity is also controlled by factors like the material of the particles, the size dependent aggregation and clustering of the nanoparticles, the size and shape of the nanoparticles. Particle size is an important parameter for controlling the thermal properties of nanofluids. Earlier we have investigated the size dependence on optical nonlinearities of the Ag and thermal diffusivity of Au nanoparticles prepared by gamma irradiation in PVP solution [17-20]. In this paper, we studied the thermal diffusivity of Ag nanoparticles prepared by UV irradiation in order to see the effect of particle size and preparation method on thermal properties of colloidal solutions.

2. Experimental

In this work, we used $AgNO_3$ (99.98%) from Merck, Germany, as silver precursor and polyvinylpyrrolidone (PVP) (MW 29,000, Aldrich) as a colloidal stabilizer. For preparing Ag nanofluid samples, 3 g of PVP and 1 mL of isopropanol as hydroxyl radical scavenger were used. At first, the PVP powder was dissolved in 50 ml distilled in ambient temperature. Then to remove oxygen, the solution was bubbled by nitrogen gas (99.5%) and stirred around 3 hours. The 50 mg of $AgNO_3$ (5.88×10^{-3} M) has been added into PVP solution and the prepared solution was stirred again for 4 hours more to acquire PVP/$AgNO_3$ sol. A UV reactor was used for irradiation the PVP/$AgNO_3$ solution in different times at wavelength of 365 nm while the solution is rotated at speed of 195 rpm by a magnetic stirrer. The irradiation times of 2 h (S1), 4 h (S2), 10 h (S3), 35 h (S4) and 60 h (S5) were utilized respectively for different cells. In this level, UV-Irradiation creates hydrated electrons which reduce the Ag ions to Ag atoms in solution.

A UV-Vis spectrometer (Lambda 25 – Perkin Elmer) was used to characterize of plasmon peak of distributed Ag nanoparticles inside the solutions. The average size of Ag nanoparticles was measured by a nanophox machine (Sympatec GmbH, D-38678).

Both, the shape and the polydispersivity of each sample, was determined through transmission electron microscopy (TEM). The structure of Ag/PVP has been investigated using X-Ray Diffraction (XRD). The XRD analysis was done by a Philips PW-3050 with copper tube operated at 40 kV and 40 mA. Data was taken for 2θ range of 30 to 85 degrees with a step of 0.02 degree. All XRD measurements were recorded at ambient temperature.

Fig. 1 shows the schematic diagram of the TLS experimental setup. The setup includes a diode laser at wavelength of 532 nm with 60 mW output power and a He- Ne laser (HRP050) at 0.5 mW as a probe beam. A chopper (SR540) was applied to modulate the light excitation beam. The excitation beam onto cuvette samples was focused by a lens of 21 cm focal length. The probe beam at angle of around 1.5 degree with respect to diode laser beam passed through to the lens of 5 cm focal length and liquid samples then collected by a photodiode detector (PD) after going through band pass filter. A digital oscilloscope (Tektronix TD 210) was used to record the signal and storage the data. The TL data from oscilloscope was captured and analyzed by LABVIEW software and then normalized with respected to thermal lens signal at time t=0.

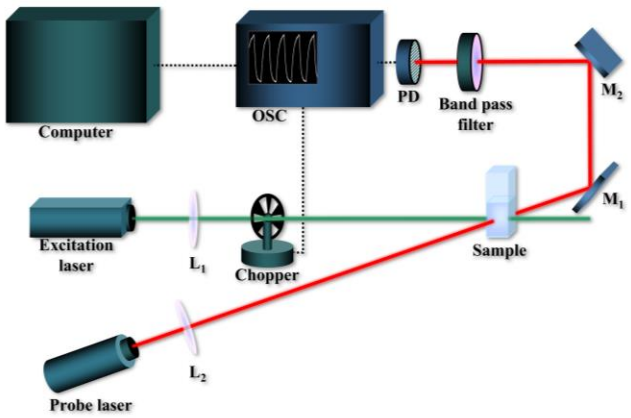

Fig. 1. The TL experimental set-up

3. Theory

The normalized transmitted probe beam at far field as a function of time can be calculated from the Shen formula which is derived for Gaussian beams in 1995 [21]. The transmission beam located at the far field respect to Rayleigh parameter and centered at the beam axis. The TL relation is given by:

$$I(z,t) = I_0\left(1-\theta\tan^{-1}\left(\frac{2mV}{[(1+2m)^2+V^2]\frac{t_c}{2t}+1+2m+V^2}\right)\right)^2 \quad (1)$$

where

$$V = Z_1/z_C;\quad m=\left(\frac{\omega_p}{\omega_e}\right)^2;\quad t_c=\frac{\omega_e^2}{4D},\quad \theta=\frac{P_e.\alpha.l}{\kappa\lambda_P}\frac{ds}{dT} \quad (2)$$

in which Z_1 is the distance from samples to beam waist point, $z_C=\omega_0^2/\lambda$ is the confocal distance, ω_0 is the probe beam waist radius, $\lambda=\lambda_p$ is the probe beam wavelength, ω_p and ω_e are the beam waists of probe and excitation lasers at samples, respectively. D is the thermal diffusivity and K is the thermal conductivity of samples. p_e is the beam power of excitation laser, α is the absorption coefficient, L is the length of sample. I_0 is initial intensity of $I(t)$ at t=0 and $I(t)$ is the probe beam intensity at time of t. the time constant t_c, is the characteristic thermal parameter which shown in Eq. (1). The ds/dT is the change in optical path length versus temperature at the probe beam and can be written as [22]:

$$\frac{ds}{dT}=(n-1)(1+\nu)\alpha_T+\frac{dn}{dT} \quad (3)$$

while α_T is the linear thermal expansion coefficient, n is linear refractive index of sample, ν is Poisson ratio, and ds/dT is the change of refractive index as function of temperature change.

4. Results and discussion

4.1. Characterization

Fig. 1 shows the absorption spectra of the prepared Ag nanoparticles using different UV-irradiation times. All the measurement were performed at room temperature and for visible light in the range of 300-800 nm. The surface plasmon resonance for 60h, 35h, 10h, 4h and 2h UV irradiation, are 443.8 nm, 448 nm, 451 nm, 453 nm and 455 nm respectively. It shows that an increasing in size with decreasing the UV irradiation time on the nanofluid corresponds with the shifting of the optical absorption peak to higher wavelengths or lower energies [23]. This can be explained by the fact that with UV irradiation time increase, the photo-induced fragmentation of particles is also increased and, therefore, the size of particles decreases. On the other hand, more Ag ions have been converted to the Ag nanoparticles at higher UV irradiation time, which is consistent with the increasing of the absorption intensity [24].

Table 1. Ag/PVP nanofluid samples prepared by UV-irradiated

samples	particle size (nm)	$t_c(10^{-3}$ s)	θ	D(10^{-3} cm^2/s)
S1	18	3.461±0.05	2.31±0.03	2.94±0.13
S2	15	3.700±0.04	1.57± .02	2.75±0.11
S3	10	4.988±0.08	1.30±0.04	2.04±0.09
S4	7	5.560±0.07	1.09±0.03	1.83±0.14
S5	5	5.916±0.04	1.01±0.01	1.72±0.03

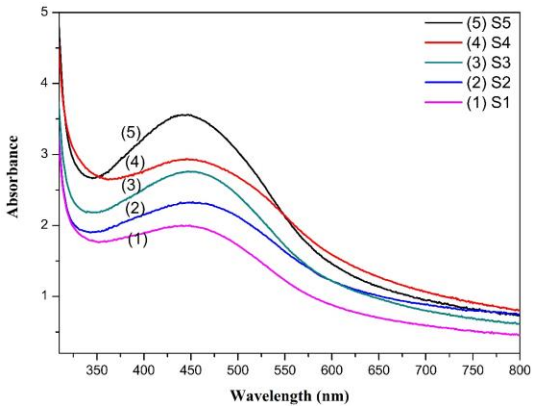

Fig. 2. Absorption spectra of Ag nanofluid at different UV irradiation time

The X-ray diffraction pattern of the prepared sample by UV irradiation at the time 4h (sample S2) is shown in Fig. 3. A number of Bragg reflections can be seen which correspond to the (111), (220) and (311). These values are compared with the JCPDS, silver file No. 04-0783 and confirm that the resultant particles are face-centered cubic (fcc) silver nanoparticles. The highest intensity in the peaks is related to face centered cubic reflection (111), which is observed in the sample. The intensity of peaks reflects the high degree of crystallinity of silver nanoparticles. The mean size of Ag nanoparticles was estimated by using Debye–Scherrer formula [25, 26]:

$$D = \frac{0.9\lambda}{\beta \cos\theta} \tag{4}$$

where λ is wave length of X-ray (0.1541 nm), β is full width at half-maximum (FWHM), θ is the diffraction angle and D is the mean particle diameter size. The calculated D from Eq. (4) is 15.06 nm.

The TEM image and corresponding size distribution of the sample S2 are displayed in Fig. 4. It can be seen that particles with mean diameter of 15.23 nm have been obtained and well dispersed in solution which avoid the effect of agglomeration of particles on thermal diffusivity measurement. The TEM data is in good agreement with the XRD results and also nanophox measurements.

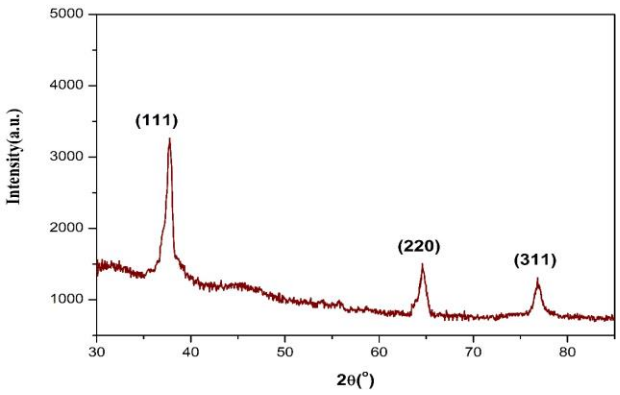

Fig. 3. X-Ray diffraction patterns of Ag/PVP nanoparticles for S2

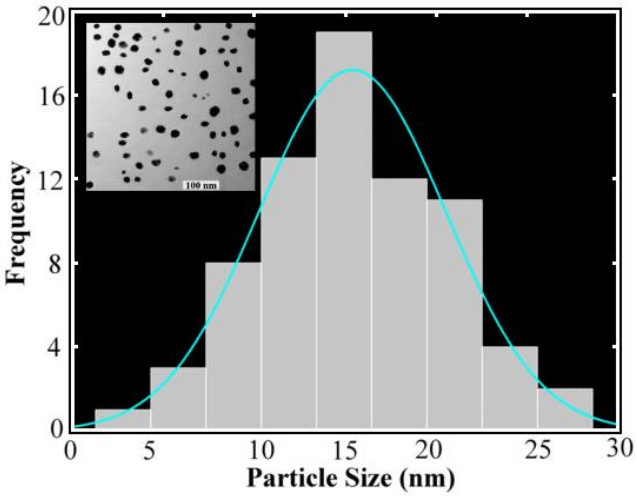

Fig. 4. Particle size distributions and TEM image of Ag/PVP for S2

4.2. Thermal diffusivity

For adjusting the TL set up, time evolution of normalized TL signal was executed for toluene (Aldrich) as a reference ad obtained data fitted to Eq. (1). The values of fitting parameters was found to be θ(5.798±0.028) and t_c(0.010±0.002s) and then the value of thermal diffusivity was calculated to be $(10.88\pm0.12)\times10^{-4}$ cm^2/s. From the literature, the thermal diffusivity of toluene has been reported as 10.90×10^{-4} cm^2/s [27]. The small difference, 0.2%, from reference reveals a good alignment and agreeable data output in present TL setup. The main source of error was mostly from the fitting.

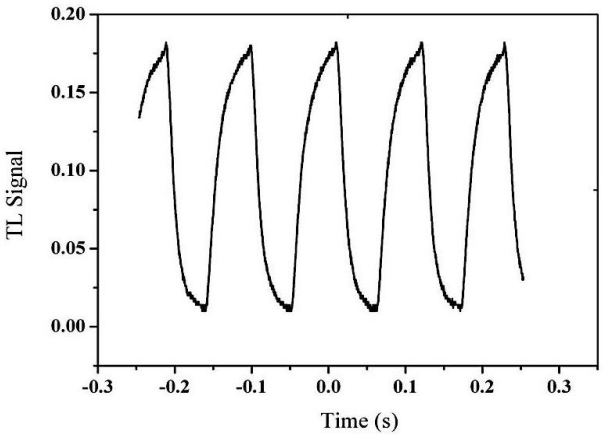

Fig. 5. TL signal of Ag/PVP at concentration of 5.88×10-3 M and irradiated at UV for 4h

Fig. 5 shows a typical TL signal as variation of time for S2. The experimental data is fitted by Eq. (1) for obtain adjustable parameters θ and characteristic thermal time constant (t_c). Then, from the Equation (1), thermal diffusivity of the sample can be easily calculated. This process was employed to all experimental data to acquire

the samples thermal diffusivity. Fig. 6 shows a typical TL signal as a function of time for sample S2. As it can be seen, the theoretical curve calculated using equation (1) successfully fitted to the experimental data and the obtained thermal diffusivity value for the sample is 2.75×10^{-3} cm^2/s.

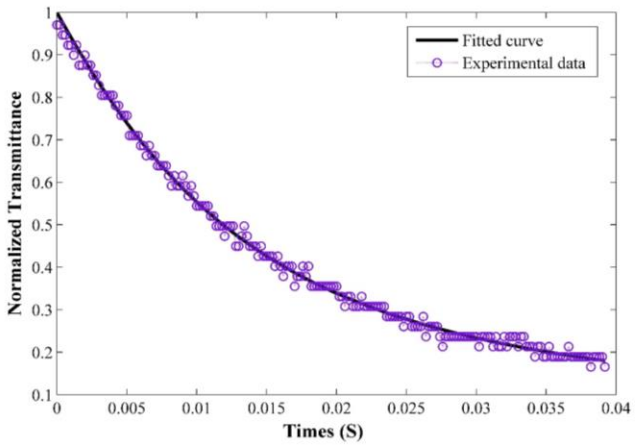

Fig. 6. Time evolution of the TL signal for Ag nanofluid (S2). Symbol (O) represents the experimental data and solid line is the fitting line to Equation (1)

The value of thermal diffusivity for other UV irradiation times was measured and listed in Table 1. The general trend in our experimental data is that the thermal diffusivity of Ag nanofluids increases with increasing particle size (Fig. 7). There is also reported result of an increase in thermal diffusivity with increasing particle size for CdS nanoparticles dispersed in solution [28]. This increment can be due to thermal resistant between nanoparticles and surrounding liquid which scatters thermal waves (phonons). Given that, when the size of particles becomes smaller, the phonon dispersion carries over less energy to surrounding medium [29]. Moreover, the stored energy in phonon modes is consecutively transferred to the solution.

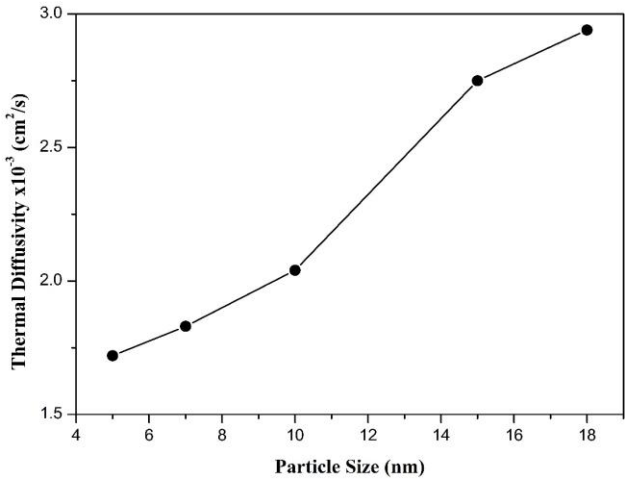

Fig. 7. The variations of thermal diffusivity of Ag nanoparticles as a function of particle size

5. Conclusion

In summary, UV irradiation method described in this article provides size controllable synthesis of high quality Ag nanoparticles in PVP solution. The average size of Ag nanoparticles was measured by a nanophox machine and by transmission electron microscopy (TEM). The structure of Ag/PVP has been investigated using X-Ray Diffraction (XRD). We measured thermal diffusivity of Ag nanofluids containing particles with different sizes prepared by the UV irradiation. Our results showed that thermal diffusivity of the fluid increases when the size of the particles is increased. We attributed this decrement in thermal diffusivity to phonon scattering at interface of particles–liquid and poor contact between the nanoparticles and surrounded liquid. As the particle size decreases, the phonon scattering transfers less energy to the surrounding liquid, which leads to a reduction in the thermal diffusivity.

Acknowledgements

We gratefully acknowledge the nano research center of Shahrekord University for providing the research facilities to enable us to carry out this research.

References

[1] A. Vaseashta, J. Irudayaraj, J. Optoelectron. Adv. M. **7**, 35 (2005).
[2] S. W. Koch, A. Knorr, Science **293**, 2217 (2001).
[3] D. P. O. Neal, L. R. Hirsch, N. J. Halas, et al., Cancer Lett. **209**, 171 (2004).
[4] D. S. Wen, W. Ding, IEEE Trans. Nanotech. **5**, 220 (2006).
[5] S. P. Jang, S. U. S. Choi, Appl. Therm. Eng. **26**, 2457 (2006).
[6] K. Hamad-Schifferli, J. Schwartz, A. T. Santos, et al., Nature **415**, 152 (2002).
[7] C. Loo, A. Lin, L. Hirsch et al., Tech. Cancer Res. Treat. **3**, 33 (2004).
[8] M. Darroudi, M. B. Ahmad, R. Zmiri, et al., J. All. Comp. **509**, 1301 (2011).
[9] R. Zamiri, B. Z. Azmi, H. Abbastabar, et al., Bull. Mat. Sci. **35**, 727 (2012).
[10] R. Zamiri, B. Z. Azmi, M. Darroudi, Appl. Phy. A **102**, 189 (2011).
[11] M. Darroudi, M. B. Ahmad, K. Shameli, et al., Solid State Sci. **11**, 1621 (2009).
[12] S. Bialkowski, Photothermal Spectroscopy Methods for Chemical Analysis Wiley New York (1996).
[13] J. Shen, R. D. Lowe, R. D. Snook, Chem. Phys. **18**, 403 (1996).
[14] J. L. J. Perez, R. G. Fuentes, J. F. S. Ramirez, A. C. Orea, Eur. Phys. J. Spec. Top. **153**, 159 (2008).
[15] J. L. J. Perez, R. G. Fuentes, E. M. Alvarad, et al., Appl. Surf. Sci. **255**, 701 (2008).
[16] Q. Xue, W. M. Xu, Mater. Chem. Phys. **90**, 298

(2005).
[17] E. Shahriari, W. M. M. Yunus, K. Naghavi, J. Optoelectron. Adv. M. **12**(8), 1676 (2010).
[18] E. Shahriari, W. M. M. Yunus, J. Optoelectron. Adv. M. **12**, 2306 (2010).
[19] E. Shahriari, W. M. M. Yunus, K. Naghavi, R. Zamiri, J. Europ. Opt. Soc. Rap. Public. **8**, 13026 (2013).
[20] E. Shahriari, W. M. M. Yunus, E. Saion, Braz. J. Phy. **40**, 256 (2010).
[21] J. Shen, R. D. Lowe, R. Snook, Chem. Phys. **18**, 403 (1998).
[22] A. A. Andrade, T. Catunda, Rev. Sci. Inst. **74**, 877 (2003).
[23] K. Naghavi, E. Saion, W. M. M. Yunus, Radiat. Phys. Chem. **79**, 1203 (2010).
[24] C. F. Bohren, D. R. Huffman, John Wiley & Sons Inc. New York (1998).
[25] S. S. Nath, D. Chakdar, G. Gope, Nano Trends: J Nanotechnol Appl. **2**, 3 (2003).
[26] B. D. Hall, D. Zanchet, D. Ugarte, J. Appl. Cryst. **33**, 1335 (2000).
[27] R. C. Weast, CRC Handbook of Chemistry and Physics CRC Press Boca Raton FL (1987).
[28] A. Zakaria, R. Zamiri, P. Vaziri, et al., World Acad. Sci. Eng. Tech. **55**, 92 (2011).
[29] Z. B. Ge, D. G. Cahill, P. V. Braun, Phys. Rev. Lett. **96**, 186101 (2006).

*Corresponding author: esmaeil.phy@gmail.com